

# Accepted Manuscript

Rapid solid-phase syntheses of a peptidic-aminoglycoside library

Casey Kukielski, Krishnagopal Maiti, Sayantan Bhaduri, Sandra Story, Dev P. Arya



PII: S0040-4020(18)30809-3

DOI: [10.1016/j.tet.2018.07.012](https://doi.org/10.1016/j.tet.2018.07.012)

Reference: TET 29672

To appear in: *Tetrahedron*

Received Date: 24 April 2018

Revised Date: 3 July 2018

Accepted Date: 5 July 2018

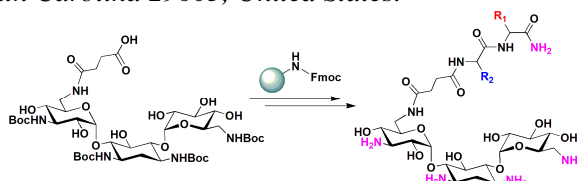
Please cite this article as: Kukielski C, Maiti K, Bhaduri S, Story S, Arya DP, Rapid solid-phase syntheses of a peptidic-aminoglycoside library, *Tetrahedron* (2018), doi: 10.1016/j.tet.2018.07.012.

This is a PDF file of an unedited manuscript that has been accepted for publication. As a service to our customers we are providing this early version of the manuscript. The manuscript will undergo copyediting, typesetting, and review of the resulting proof before it is published in its final form. Please note that during the production process errors may be discovered which could affect the content, and all legal disclaimers that apply to the journal pertain.

## Graphical Abstract

**Rapid Solid-phase Syntheses of a Peptidic-Aminoglycoside Library**Casey Kukielski<sup>a</sup>, Krishnagopal Maiti<sup>a</sup>, Sayantan Bhaduri<sup>b</sup>, Sandra Story<sup>b</sup> and Dev P Arya<sup>a,b,\*</sup><sup>a</sup>Laboratory of Medicinal Chemistry, Department of Chemistry, Clemson University, Clemson, South Carolina 29634, United States<sup>b</sup>NUBAD, LLC, Greenville, South Carolina 29605, United States.

Leave this area blank for abstract info.





Tetrahedron  
journal homepage: www.elsevier.com



## Rapid Solid-phase Syntheses of Peptidic-Aminoglycoside Library

Casey Kukielski<sup>a</sup>, Krishnagopal Maiti<sup>a</sup>, Sayantan Bhaduri<sup>b</sup>, Sandra Story<sup>b</sup>, and Dev P Arya<sup>a,b,\*</sup>

<sup>a</sup>Laboratory of Medicinal Chemistry, Department of Chemistry, Clemson University, Clemson, South Carolina 29634, United States

<sup>b</sup>NUBAD, LLC, Greenville, South Carolina 29605, United States

\*Corresponding author. Tel.: (864) 656-1106; fax: +0-000-000-0000; e-mail: dparya@clemson.edu

### ARTICLE INFO

### ABSTRACT

#### Article history:

Received

Received in revised form

Accepted

Available online

A library of mono- and di-amino acid peptidic-aminoglycosides (PAs), with kanamycin and neomycin as the model aminoglycosides, was systematically and rapidly synthesized via solid phase peptide synthesis. Aminoglycosides were first converted into *N*-Boc protected carboxylic acids and fourteen L-amino acids were then used in the diversification of the full library. The approach outlined describes a rapid synthetic procedure where >200 PA compounds can be synthesized in a few months with 85-95% purity. UV thermal denaturation assessed the binding stabilization by PAs to model human and bacterial A-site rRNA sequences. Significant differences were found in thermal melting profiles among PAs that were attributed to specific amino acid sequences. Neomycin PAs lead to a much larger variation in the stabilization of A-site rRNA sequences ( $\Delta T_m = 2.6-17.1$  °C) as compared to kanamycin PAs ( $\Delta T_m = 0.4-4.3$  °C). Kanamycin PAs had little activity against Gram-negative and Gram-positive bacteria as compared with neomycin PAs that had significant antibacterial activity with MIC ranging from 2 – 16  $\mu$ M.

#### Keywords:

Aminoglycoside

Deoxystreptamine

Kanamycin

Neomycin

Peptidic library

### 1. Introduction

Aminoglycosides have been at the forefront of antimicrobial therapy for the past seven decades. In addition to their use as antibiotics for the treatment of Gram-positive and Gram-negative bacterial infections, aminoglycosides are useful as scaffolds for the recognition of nucleic acids.<sup>1,2,3</sup> Aminoglycosides bind to the A-site of the 16S bacterial ribosomal RNA (rRNA) and perturb protein synthesis causing mistranslation.<sup>4</sup> Prevalent use of aminoglycosides provides the selective pressure for the development of resistance via aminoglycoside modifying enzymes (AMEs) and more recently, target mutations such as rRNA methylation.<sup>5</sup> Various chemical modifications have been reported to address the issues of aminoglycoside resistance and target recognition of the bacterial 16S rRNA. The conjugation of peptides and aminoglycoside has been reported to show evasion of action of AMEs by circumventing AME modification of the aminoglycoside core unit in addition to building unique scaffolds for RNA and DNA recognition. We report herein solid phase chemical synthesis to gain rapid access to structurally well-defined aminoglycoside-peptide conjugate library, with kanamycin and neomycin serving as model aminoglycosides. Coincident binding of peptide and aminoglycoside to rRNA may further the diversity of RNA stabilization that can be achieved using different amino acid combinations. In general, the centrally located scaffold present in most of the clinically important aminoglycoside antibiotics is the 2-deoxystreptamine (DOS) moiety<sup>6</sup> (Figure 1).

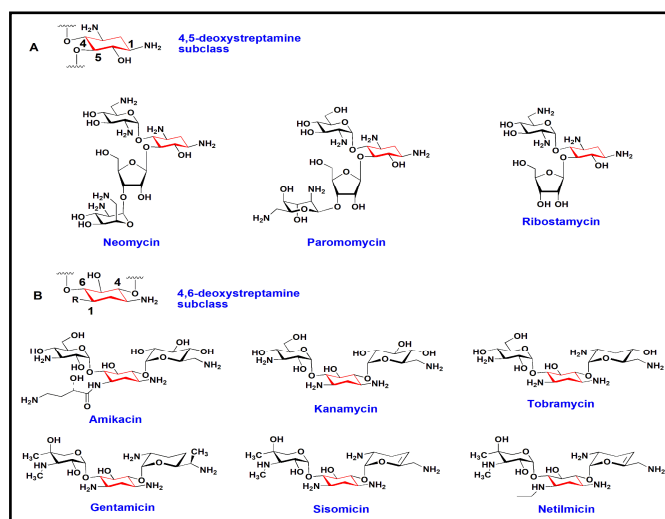


**Figure 1.** A. 4,5-deoxystreptamine subclass (neomycin, paromomycin, ribostamycin); B. 4,6-deoxystreptamine subclass (amikacin, kanamycin, tobramycin, gentamicin, sisomicin, netilmicin).

Based on the substitution pattern of the 2-DOS ring, aminoglycosides are broadly divided into two different subclasses, the 4,5- and 4,6-disubstituted DOS. Neomycin and paromomycin belong to 4,5-disubstituted subclass and

kanamycin, tobramycin, amikacin, belong to 4,6-disubstituted Minoamicin subclass (Figure 1).

To circumvent issues of aminoglycoside resistance, chemical modification of aminoglycosides has been used as a viable strategy, with a new drug plazomicin<sup>7</sup> recently receiving FDA approval. Major challenges associated with chemical syntheses of aminoglycoside-based novel antibiotics mirror the inherent difficulties related to synthesis and purification of pure and structurally well-defined carbohydrates. Challenges include: (i) the presence of multiple hydroxy and amino groups with comparable reactivity (ii) regio- and stereoselective glycosidic bonds (iii) multi-step building block synthesis (iv) the need for manipulation of numerous protecting groups and (v) tedious column purification for multiple intermediates. Therefore, due to the structural diversity of natural aminoglycosides, synthesis of modified aminoglycoside libraries remains an arduous challenge. A common strategy employed over the past decade has been to maintain the core aminoglycoside scaffold and incorporate additional binding/recognition moieties to synthesize structural analogs of natural aminoglycoside antibiotics.

Various synthetic protocols for the production of 5'-modified neomycin class of aminoglycosides have been reported for modification of antibacterial activity and nucleic acid binding.<sup>8-24</sup> Optimization of nucleic acid binding has been achieved by conjugating (via C5'-OH modification) B-DNA minor groove binding ligand Hoechst 33258<sup>25-27</sup> and intercalators such as fluorescein,<sup>28-30</sup> pyrene,<sup>31-34</sup> naphthalene diimide, anthraquinone,<sup>35, 36</sup> methidium carboxylic acid<sup>37</sup> for selective recognition of A- and B-form DNA and binding to different nucleic acid structures.<sup>38</sup> Novel perylene-neomycin conjugates have been utilized for selective targeting of nucleic acid structures such as human telomeric G-quadruplex DNA through base stacking and groove recognition.<sup>39</sup> Various triazole linked neomycin dimers and benzimidazole-neomycin conjugates through C5'-OH group modification with varying linker length have been used for selective recognition of quadruplex,<sup>40</sup> duplex RNA,<sup>41, 42</sup> miRNA,<sup>43</sup> HIV TAR-RNA.<sup>44-47</sup> Moreover, various neomycin B dimers tethered via triazole, urea and thiourea linkages were found to be poor substrates for AMEs and selectively bind bacterial A site rRNA over human A site rRNA.<sup>48, 49</sup> Nucleic acid binding chains such as PNA and DNA can be included in these target binding approaches.<sup>50-52</sup> These reports suggest that improvements in rRNA recognition can be attained by chemical modifications of naturally-occurring aminoglycosides.

Most of the synthetic approaches described above are performed using solution-phase synthesis. Compared to solid-phase synthesis, solution-phase synthesis is a slow process as it involves multiple purification steps during the course of synthesis. Thus, a methodology for rapid production of compound libraries followed by antibacterial screening and ribosomal binding analysis is highly desirable. We recently published a comprehensive approach for studying rRNA binding affinity and antibacterial activity of peptidic-neomycin library to identify novel rRNA binding antimicrobials.<sup>53</sup> Several PAs were quickly identified that bind with high affinity and greater selectivity to the *E. coli* A-site rRNA than the parent aminoglycoside as compared to the mammalian A-site. These promising results led us to expand the approach to include PAs using kanamycin, which belongs to 4,6-deoxystreptamine subclass. Herein, we successfully report the solid-phase assisted rapid synthesis of a 210 member mono- and diamino-cid peptidic-kanamycin library by using fourteen L-amino acids. A comparison of NMR spectra of neomycin and kanamycin conjugates with their precursor acid and PA derivative is

included to identify the effect of these modifications on the electronics of the parent ring structure. We also report the antibacterial activity of select kanamycin and neomycin PAs and their effects upon binding human and *E. coli* A-site rRNA as evaluated by UV thermal denaturation.

## 2. Results and discussion

### 2.1. Synthetic strategy

Retrosynthetic analysis of covalently linked peptidic-kanamycin library is given in Figure 2. The scheme is designed as a combination of both solid and solution phase synthesis.

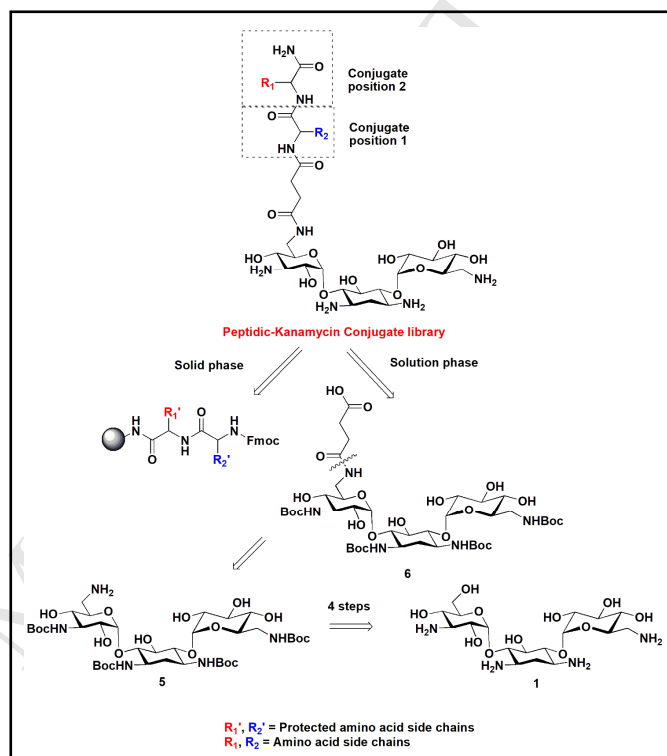


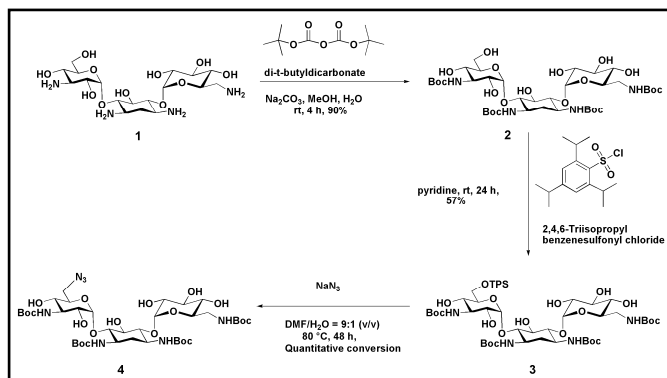
**Figure 2.** Retrosynthesis of peptidic-kanamycin conjugate library.

In solution phase, kanamycin acid monomer **6**, as the precursor for solid phase synthesis, could be synthesized from kanamycin amine **5**, which in turn can be formed from commercially available kanamycin A, **1** in 4 steps. Simultaneously, different mono- and di- amino acid conjugates could rapidly be synthesized by modifying the standard 9-fluorenylmethoxycarbonyl (Fmoc)-based solid phase peptide synthetic strategy.<sup>54</sup> Amino acid conjugates can then be coupled with kanamycin acid monomer **6**, followed by global deprotection to achieve a large PA library. The solid phase synthesis was carried out using Fmoc-PAL-PEG-PS resin by modifying Fmoc-based solid phase peptide synthetic strategy as described in the results and discussion section. This modified solid phase strategy could potentially be employed for the rapid synthesis of large libraries consisting of various Fmoc-protected amino acids, and various aminoglycosides by reducing the time and manual labor drastically. PAs were synthesized on the resin beads using HCTU (2-(6-Chloro-1H-benzotriazole-1-yl)-1,1,3,3-tetramethylammonium hexafluorophosphate) as coupling reagent and DIPEA (*N,N*-Diisopropylethylamine) as base. Successful global deprotection was achieved by using TFA (trifluoroacetic acid)/*m*-cresol (8/2 v/v) mixture. All these conjugates were synthesized (as shown in the schemes below) and characterized

by NMR spectroscopy and mass spectrometry (MALDI-TOF) as reported in the supporting information.

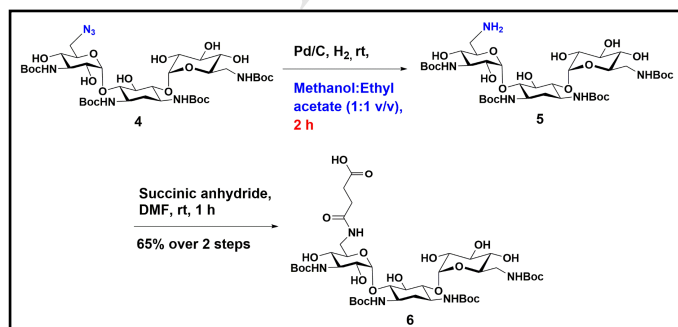
## 2.2. Synthesis of kanamycin/neomycin acid derivative

In order to synthesize peptidic-kanamycin conjugates, our first goal was to prepare kanamycin acid derivative **6**, which was initiated by selective protection of amino groups in kanamycin A, **1** with tert-butoxycarbonyl (Boc) groups to obtain **2** as shown in **Scheme 1**.



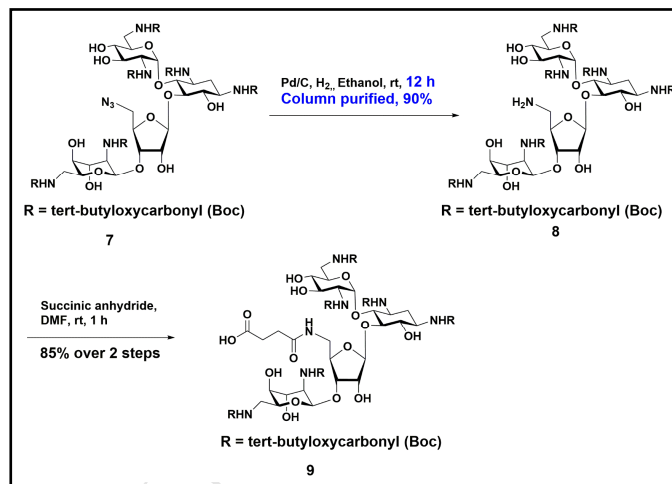
**Scheme 1.** Solution-phase synthesis of Kanamycin-azide **4**.

The primary hydroxy group (6''-OH of ring III) of compound **2** was then selectively protected with 2,4,6-triisopropylbenzenesulfonyl group, which was further substituted by azide group via  $S_N2$  displacement reaction in order to achieve the kanamycin azide derivative **4**. Hydrogenation of azide derivative furnished 6''-deoxy-6''-amino kanamycin **5** which was reacted with succinic anhydride to yield the amide bond linked kanamycin acid derivative **6** as shown in **Scheme 2**. Using solvent conditions of methanol : ethyl acetate (1:1, v/v) which completely solubilized kanamycin azide **4**, reduction was performed, and the reaction was monitored hourly after the addition of Pd/C mixture. TLC showed ~80% conversion after 1 h and complete conversion of **4** to **5** after 2 h. A quick filtration to avoid the amine exposure to atmosphere was performed to remove excess Pd/C and then dried under vacuum for 1 h. The product **5** was then immediately reacted with succinic anhydride in order to afford the final product, i.e., kanamycin acid derivative **6**. Measured amount (1.05 equiv.) of succinic anhydride was added in the reaction mixture to get quantitative conversion of the amine **5** to the corresponding acid **6** and to avoid formation of any undesired kanamycin dimer adducts (**Scheme 2**). Compound **6** was purified by extraction with water and ethyl acetate and no column chromatography was performed. The presence of a free carboxyl functional group in **6** allows us to use this key intermediate for further modifications using solid phase peptide chemistry.



**Scheme 2** Synthesis of kanamycin acid derivative **6**, the precursor for solid phase synthesis of kanamycin conjugates.

In comparison, neomycin amine **8** (**Scheme 3**) was obtained after hydrogenation of neomycin azide **7** for 12 h, followed by filtration and column purification to afford amine **8** in 90% yield. Neomycin amine **8** was further reacted with succinic anhydride to furnish the neomycin acid derivative **9**, in good yield.



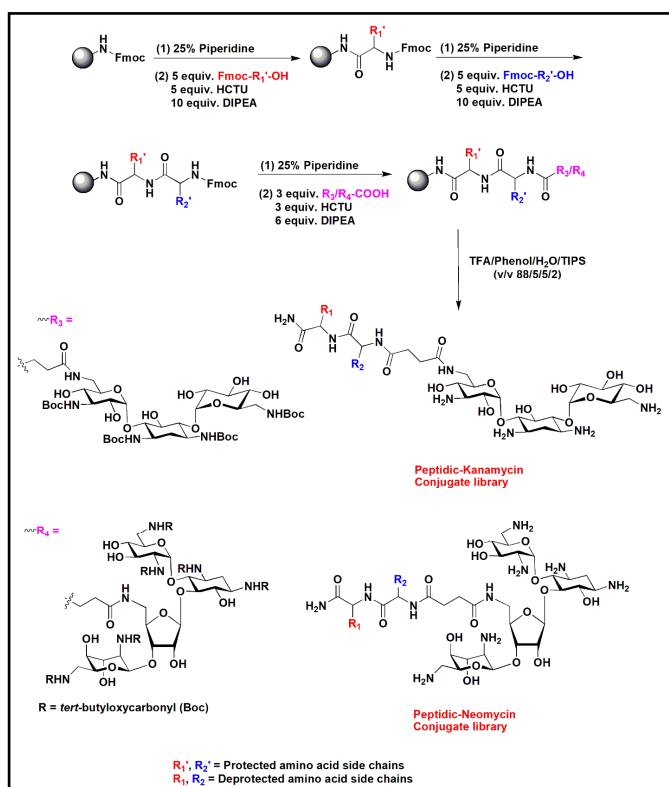
**Scheme 3.** Synthesis of neomycin acid monomer **9**: Precursor for solid phase synthesis of neomycin conjugates.

## 2.3. Synthesis of kanamycin/neomycin peptidic conjugates

With the kanamycin/neomycin acid monomers **6** and **9** in hand, the solid phase synthesis of the peptidic-kanamycin or neomycin library was carried out using Fmoc-PAL-PEG-PS resin by modifying Fmoc-based solid phase peptide synthetic strategy as shown in **Scheme 4**. The general protocol for solid-phase synthesis of peptidic-kanamycin library is detailed in the supporting information. This modified solid phase strategy was successfully employed for the rapid syntheses of a 210-member library consisting of mono- and diamino acid-kanamycin conjugates (DPA **1900-2110**) and neomycin conjugates (DPA **1167**, **1261**, **1267**, **1276** and **1281**) (shown in the supporting information) by reducing the manual labor needed in solution phase synthesis. Fifteen L-amino acids ( $\beta$ -alanine, arginine, asparagine, aspartic acid, cysteine, histidine, leucine, phenylalanine, proline, serine, threonine, tryptophan, tyrosine, lysine and valine) were studied in the full library. Growing peptide chain was attached to Fmoc-PAL-PEG-PS resin via amide linkage. Kanamycin/neomycin acid derivative **6** and **9** were coupled with different mono- and diamino acid conjugates on the resin beads using HCTU (2-(6-Chloro-1H-benzotriazole-1-yl)-1,1,3,3-tetramethylammonium hexafluorophosphate) as coupling reagent and DIPEA (*N,N*-Diisopropylethylamine) as base.

With the initial success, our next goal was removal of all molecules from the solid support and global deprotection to achieve peptidic-kanamycin/neomycin conjugate libraries. Successful global deprotection and cleavage from the solid support was accomplished by using a mixture of TFA (trifluoroacetic acid)/Phenol/water/TIPS (triisopropylsilane) (88/5/5/2 v/v). The detailed experimental procedures and characterization data (NMR and MALDI-TOF) of all the compounds are shown in the supporting information. Complete characterization including  $^1\text{H}$ ,  $^{13}\text{C}$  NMR and MALDI were

performed on ten compounds, DPA 1167, 1261, 1267, 1276, 1281, 1966, 2060, 2066, 2075 and 2081 (Figure 3).



**Scheme 4.** Solid-phase syntheses of peptidic-kanamycin/neomycin conjugates.

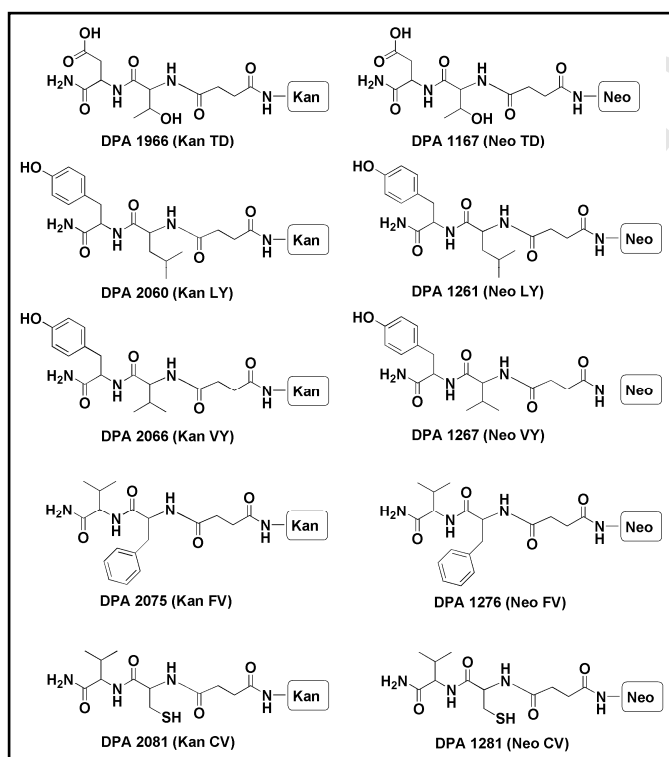
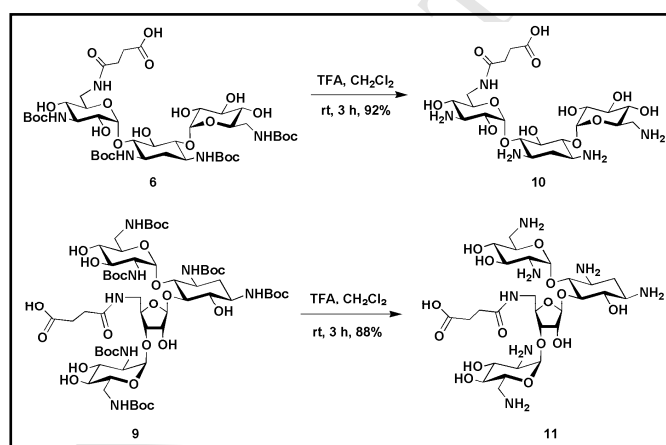


**Figure 3.** Solid-phase syntheses of peptidic-kanamycin/neomycin conjugates: Some of the representatives are shown such as DPA 1167, 1261, 1267, 1276, 1281, 1966, 2060, 2066, 2075 and 2081.

## 2.4. Synthesis of deprotected kanamycin/neomycin acid derivative

In order to perform comparative NMR studies of the synthesized kanamycin/neomycin conjugates with their precursor acid derivatives, deprotection (removal of tert-butyloxycarbonyl groups) of kanamycin and neomycin acid derivatives (**6** and **9**) was carried out in the presence of trifluoroacetic acid (TFA) to obtain the corresponding deprotected kanamycin and neomycin acid derivatives **10** and **11** (Scheme 5). The formation of compounds **10** and **11** was confirmed by NMR spectroscopy and mass spectrometry (MALDI-TOF). The characterization data are shown in the supporting information.



**Scheme 5.** Synthesis of deprotected kanamycin and neomycin acid derivative.

## 2.5. NMR studies of kanamycin/neomycin conjugates with their precursor acid derivative

A comparative study of the synthesized kanamycin and neomycin conjugates with their corresponding acid precursor were then undertaken by NMR spectroscopy. The protons of aminoglycoside kanamycin A and neomycin B were assigned and confirmed as known in the literature.<sup>55, 56</sup> We first assigned anomeric protons and carbons for the acid derivative **10** and **11** by using 2D NMR spectroscopy. The HMQC (<sup>1</sup>H-<sup>13</sup>C 2D NMR) spectra for the compound **10** and **11** are shown in Figure 4 and 5, respectively. For clarity, we designated the cyclic rings for both the systems (kanamycin and neomycin) as I-IV as shown in the Figure 6. In <sup>1</sup>H NMR spectrum of kanamycin acid derivative **10**, anomeric protons for the ring III and II appeared at 5.09 ( $J = 3.3$  Hz) and 5.68 ppm ( $J = 3.9$  Hz), as a doublet, respectively. The anomeric carbons for the ring III and II in compound **10**, appeared at 100.7 and 96.8 ppm, respectively, in <sup>13</sup>C NMR spectrum of **10**. On the other hand, the anomeric protons for the pyranosyl ring II and IV in neomycin acid derivative **11**, resonated at 5.89 and 5.26 ppm as an apparent singlet, respectively, whereas the anomeric proton of furanoside ring III appeared at 5.34 ppm as a doublet ( $J = 3.6$  Hz), in the <sup>1</sup>H NMR spectrum of **11**. In <sup>13</sup>C NMR spectrum of **11**, anomeric carbons for the pyranosyl ring II and IV appeared at 94.9 and 95.7 ppm, respectively, whereas the anomeric carbon for the furanoside ring III resonated at 109.13 ppm in <sup>13</sup>C NMR spectrum of **11**.

Based on the assignment of anomeric protons and carbons of kanamycin and neomycin acid derivative, we similarly assigned the chemical shifts of their amino acid components. The 2D NMR spectra (HMQC) of the conjugates are shown in the supporting information. Comparative NMR studies were carried out with the PAs and their precursor acid derivative and

kanamycin/neomycin sulphate and are given as stack plots of  $^1\text{H}$  NMR spectra (Figures 7 and 8).

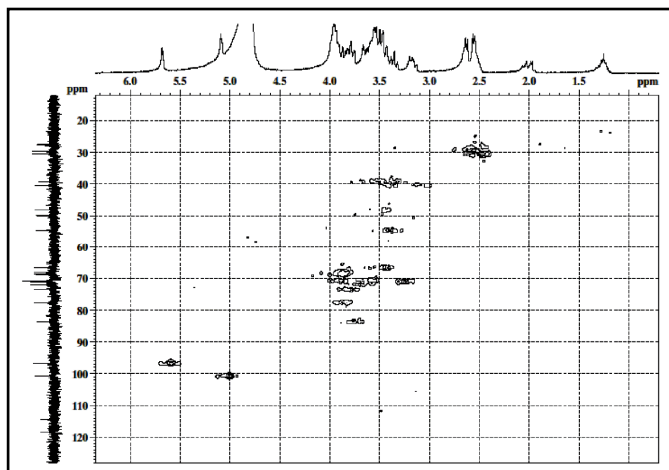


Figure 4. HMQC spectrum kanamycin acid derivative **10**.

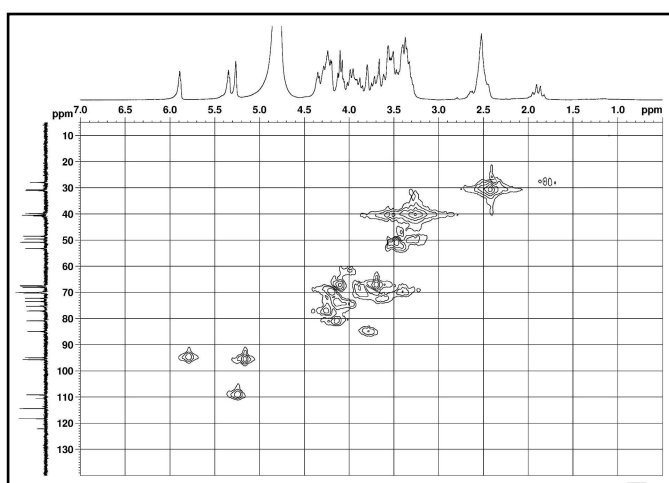


Figure 5. HMQC spectrum neomycin acid derivative **11**.

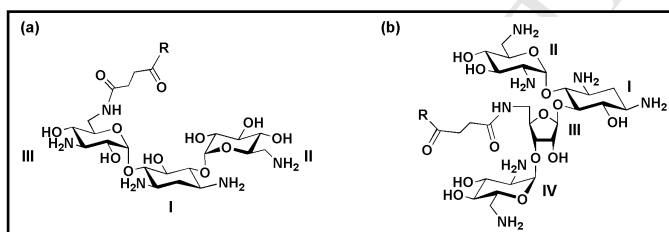


Figure 6. Structures of (a) kanamycin (a) and (b) neomycin conjugates, designated with different ring systems, where R represents hydroxy group for acid derivative; and amino acids moiety for the conjugates.

The stack plots of  $^1\text{H}$  spectra of kanamycin and neomycin PAs with their corresponding acid precursor is shown in Figure 7 and 8, respectively.

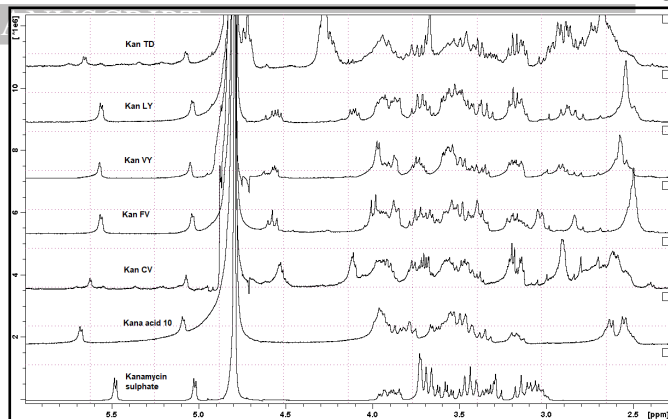


Figure 7. Stack plot for  $^1\text{H}$  NMR spectra (in  $\text{D}_2\text{O}$ ) of kanamycin sulphate, kanamycin acid derivative **10** and its various peptidic conjugates.

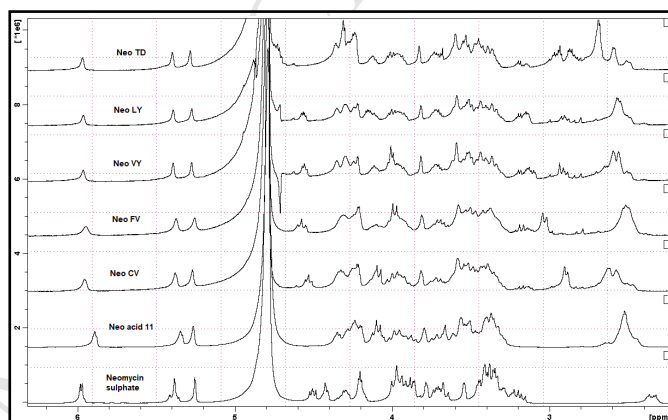


Figure 8. Stack plot for  $^1\text{H}$  NMR (in  $\text{D}_2\text{O}$ ) spectra of neomycin sulphate, neomycin acid derivative **11** and its various peptidic conjugates.

The resonance values for the anomeric protons and carbons for both kanamycin and neomycin derivatives are shown in Table 1 and 2, respectively. A small upfield shift of anomeric H1 protons of the ring II in all the kanamycin conjugates was observed as compared to its acid derivative **10**. On the other hand, a small downfield shift of anomeric H1 protons of the ring II in all the neomycin conjugates was observed as compared to its acid derivative **11**. These results suggest that for both the 4,6- and 4,5-DOS aminoglycosides, substitutions by different amino acids at the primary hydroxy group do not substantially or differentially perturb the electronics of the base rings. The amino acid chains can then be expected to interact with the enzyme or ribosomal RNA without electronically perturbing the functional groups present in the natural aminoglycosides, that are required for binding to the eubacterial rRNA A-site.

**Table 1.** Resonance values of anomeric protons and carbons of kanamycin derivatives.

Compound	Anomeric H1 for ring II (ppm)	Anomeric H1' for ring III (ppm)	Anomeric C1 for ring II (ppm)	Anomeric C1' for ring III (ppm)
Kanamycin sulphate	5.48	5.02	97.47	100.08
Kanamycin acid derivative <b>10</b>	5.68	5.09	96.77	100.70
Kan CV (DPA <b>2081</b> )	5.62	5.07	97.07	100.77
Kan FV (DPA <b>2075</b> )	5.56	5.03	97.06	100.78
Kan VY (DPA <b>2066</b> )	5.57	5.05	97.25	100.81
Kan LY (DPA <b>2060</b> )	5.56	5.04	97.27	100.81
Kan TD (DPA <b>1966</b> )	5.65	5.07	97.05	100.72

**Table 2.** Resonance values of anomeric protons and carbons of neomycin derivatives.

Compound	Anomeric H1 for ring II (ppm)	Anomeric H1' for ring III (ppm)	Anomeric H1'' for ring IV (ppm)	Anomeric C1 for ring II (ppm)	Anomeric C1' for ring III (ppm)	Anomeric C1'' for ring IV (ppm)
Neomycin sulphate	5.98	5.40	5.25	95.15	110.18	95.19
Neomycin acid derivative <b>11</b>	5.89	5.34	5.26	94.92	109.13	95.69
Neo CV (DPA <b>1281</b> )	5.96	5.38	5.27	94.89	109.39	95.77
Neo FV (DPA <b>1276</b> )	5.95	5.37	5.26	94.88	109.39	95.76
Neo VY (DPA <b>1267</b> )	5.96	5.39	5.28	94.89	109.45	95.74
Neo LY (DPA <b>1261</b> )	5.96	5.39	5.28	94.87	109.44	95.75
Neo TD (DPA <b>1167</b> )	5.97	5.40	5.28	94.88	109.40	95.73

### 2.6. Thermal denaturation analysis of kanamycin/neomycin conjugates binding human and *E. coli* A site rRNA

The effects of select kanamycin and neomycin PAs with a 27-base model of *E. coli* and human A-site rRNA (**Figure 9**) was evaluated by UV thermal denaturation. The melting temperature ( $T_m$ ) for the human and *E. coli* A-site was found to be 51.5 and 62.4 °C, respectively (**Table 3**). Kanamycin sulphate showed little change in  $T_m$  (-1 °C) upon binding to the human A site, whereas a small change in  $T_m$  (2.1 °C) when bound with the *E. coli* A site was observed (**Figure 10 and 11**). Neomycin sulphate imparted a larger change in  $T_m$  of 3.7 °C upon binding with the *E. coli* A site. Kanamycin acid derivative (**10**) and kanamycin-peptides exhibited a change in  $T_m$  that ranged from 0.4 to 2.6 °C upon binding with human A-site ( $T_m$  of 51.5 °C), where kanamycin conjugate Kan LY showed the highest  $T_m$  of 54.1 °C. A similar trend was observed with kanamycin-peptides bound to the *E. coli* A site with increases in  $T_m$  of 1.1 to 4.3 °C with Kan LY yielding the highest  $T_m$  of 66.7 °C as compared to *E. coli* A site alone ( $T_m$  of 62.4 °C). The change in  $T_m$  varied from 2.6 to 10.8 °C with neomycin acid derivative (**11**) and neomycin-

peptides when bound with the human A-site (**Figure 12**), whereas upon binding with the *E. coli* A site, the melting temperature ( $T_m$ ) was found to vary from 71.3 to 79.5 °C (**Figure 13**). In both cases for the human and *E. coli* rRNA, neomycin conjugate Neo LY exhibited the maximum increment of denaturation temperature by 10.8 and 17.1 °C, respectively. The UV thermal denaturation studies reveal that conjugation of amino acids to neomycin impart greater stabilization of both human and *E. coli* A-site rRNA as compared to the corresponding kanamycin PAs. This was most dramatic for the PAs Kan LY and Neo LY that had the greatest  $\Delta T_m$  of 4.3 °C and 17.1 °C respectively of the target rRNA structures. To the best of our knowledge, such large stabilizations of rRNA by tunable aminoglycoside variants, such as PAs shown here, have never been reported.

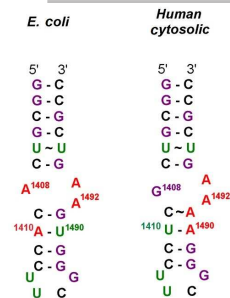


**Figure 9.** Secondary structures of the *E. coli* and human A-site rRNA models used in this study.

**Table 3.** UV melting temperature ( $T_m$ , °C) of human A-site rRNA and *E. coli* A-site rRNA bound to PAs.

$T_m$				
Human A-site rRNA		51.5		
<i>E. coli</i> A-site rRNA		62.4		
Compounds	$T_m$ human A-site	$\Delta T_m$	$T_m$ <i>E. coli</i> A-site	$\Delta T_m$
Kanamycin sulphate	50.5	-1.0	64.5	+2.1
Kanamycin acid derivative (10)	51.9	+0.4	63.5	+1.1
Kan TD (DPA 1966)	53.9	+2.4	64.4	+2.0
Kan LY (DPA 2060)	54.1	+2.6	66.7	+4.3
Kan VY (DPA 2066)	52.7	+1.2	64.8	+2.4
Kan FV (DPA 2075)	52.3	+0.8	65.0	+2.6
Kan CV (DPA2081)	52.2	+0.7	65.2	+2.8
Neomycin sulphate	50.5	-1.0	66.1	+3.7
Neomycin acid derivative (11)	57.0	+5.5	72.8	+10.4
Neo TD (DPA 1167)	61.8	+10.3	71.3	+8.9
Neo LY (DPA 1261)	62.3	+10.8	79.5	+17.1
Neo VY (DPA1267)	59.0	+7.5	76.0	+13.6
Neo FV (DPA 1276)	54.1	+2.6	72.4	+10.0
Neo CV (DPA1281)	58.4	+6.9	75.2	+12.8

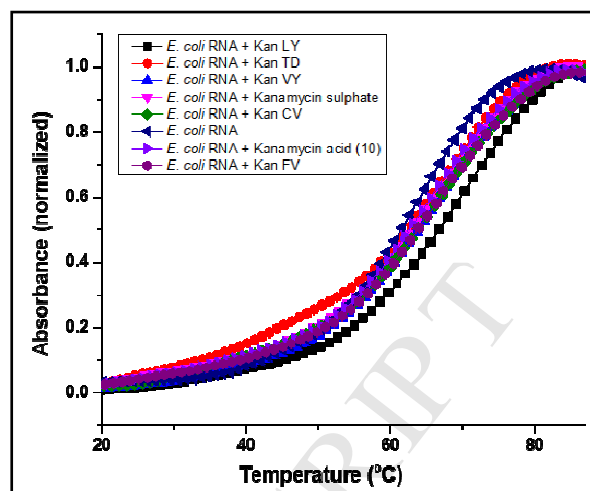


**Figure 11.** Thermal melting profiles of *E. coli* A-site rRNA upon binding with kanamycin PAs.

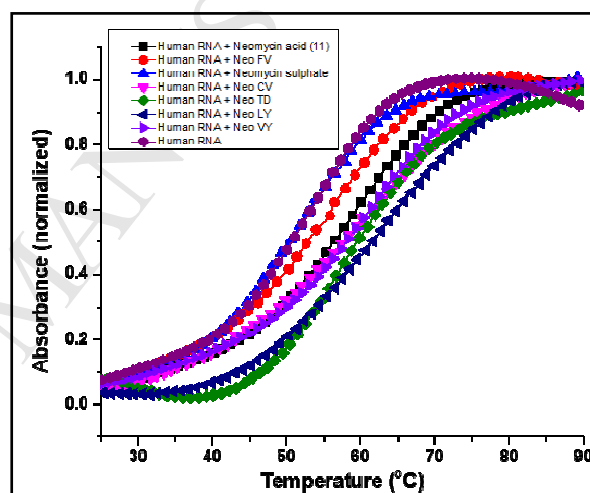


**Figure 12.** Thermal melting profiles of human A-site rRNA upon binding with neomycin PAs.

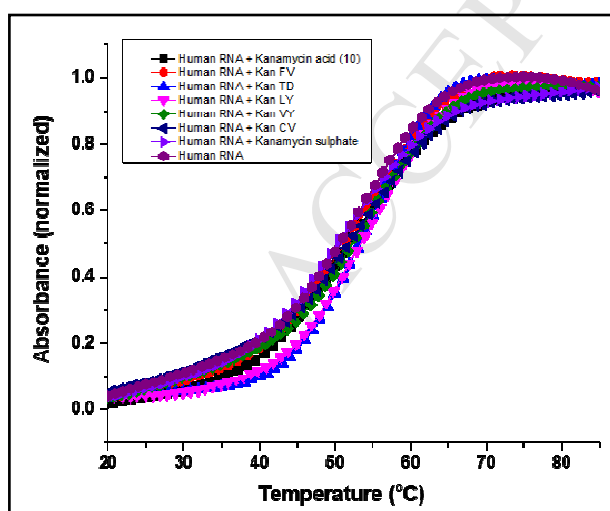


**Figure 10.** Thermal melting profiles of human A-site rRNA upon binding with kanamycin PAs.

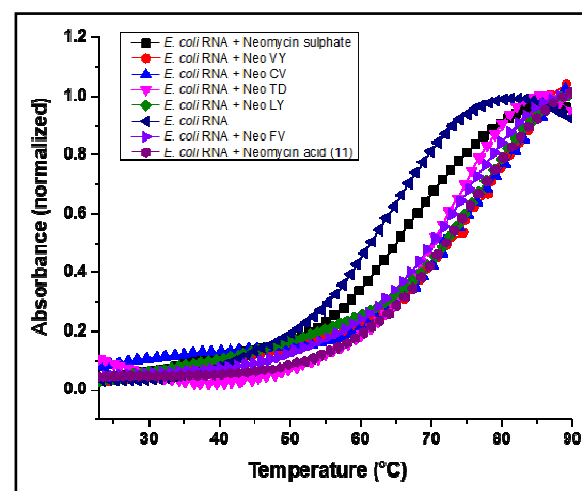


**Figure 13.** Thermal melting profiles of *E. coli* A-site RNA upon binding with neomycin PAs.

## 2.7. Antibacterial activity of kanamycin- and neomycin-PAs

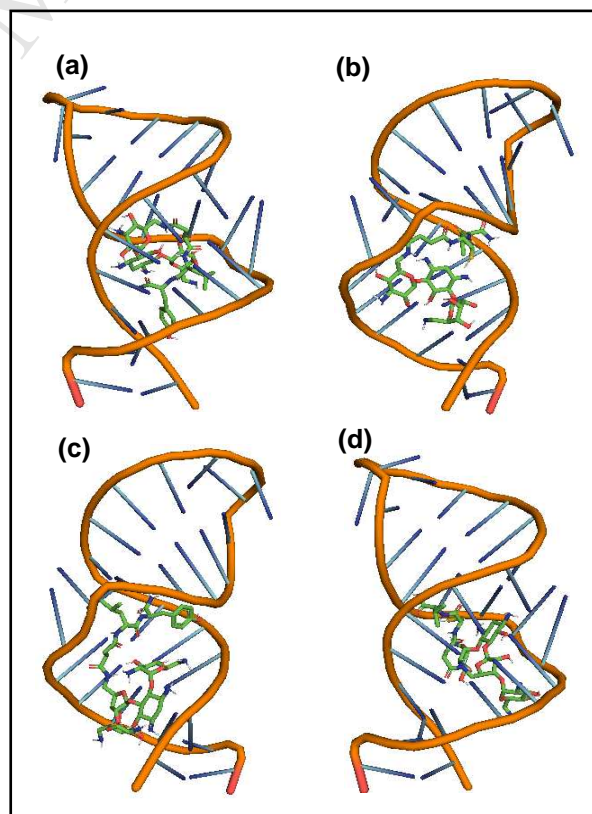
**Table 4.** Minimum inhibitory concentration (MIC  $\mu\text{M}$ ) of kanamycin and neomycin PAs against bacterial strains and (percent growth inhibition) for each bacterial strain.

DPA#	<i>E. coli</i> ATCC 25922	<i>S. aureus</i> ATCC 25923	<i>P. aeruginosa</i> ATCC 27853	MRSA ATCC 1960649
<b>MIC of Kanamycin and Kanamycin PAs</b>				
Kanamycin sulphate	4	4	>64 (11 $\pm$ 1)	>64 (25 $\pm$ 3)
Kanamycin acid derivative (10)	>64 (23 $\pm$ 2)	>64 (85 $\pm$ 10)	>64 (13 $\pm$ 1)	>64 (32 $\pm$ 3)
Kan TD (DPA 1966)	>64 (0)	>64 (0)	>64 (0)	>64 33 $\pm$ 2
Kan LY (DPA 2060)	>64 (0)	>64 (0)	>64 (0)	>64 (0)
Kan VY (DPA 2066)	>64 (0)	>64 (0)	>64 (0)	>64 (0)
Kan FV (DPA 2075)	>64 (0)	>64 (0)	>64 (0)	>64 (0)
Kan CV (DPA 2081)	>64 (19 $\pm$ 1)	>64 (40 $\pm$ 4)	>64 (0)	>64 (30 $\pm$ 6)
DPA#	<i>E. coli</i> ATCC 25922	<i>S. aureus</i> ATCC 25923	<i>P. aeruginosa</i> ATCC 27853	MRSA ATCC 1960649
<b>MIC of Neomycin and Neomycin PAs</b>				
Neomycin sulphate	2	2	>64 (52 $\pm$ 3)	>64
Neomycin acid derivative (11)	4	2	>64 (0)	64
Neo TD (DPA 1167)	64	32	>64 (0)	>64 (34 $\pm$ 2)
Neo LY (DPA 1261)	16	4	>64 (0)	>64 (30 $\pm$ 4)
Neo VY (DPA 1267)	16	4	>64 (0)	>64 (36 $\pm$ 0)
Neo FV (DPA 1276)	32	8	>64 (0)	>64 (37 $\pm$ 2)
Neo CV (DPA 1281)	8	4	>64 (14 $\pm$ 1)	>64 (52 $\pm$ 4)

Antibacterial activity for kanamycin and neomycin PAs were assessed using two Gram-positive and two Gram-negative reference strains. Similar to the effects observed in rRNA A-site stabilization, kanamycin PAs were much weaker antibacterial compounds with only DPA 2081 exhibiting significant activity against the *S. aureus* and MRSA strain (Table 4). In contrast, *E. coli* and *S. aureus* were susceptible to several of the neomycin PAs with MIC values ranging from as low as 4  $\mu\text{M}$  to 64  $\mu\text{M}$ . DPA 1281 was the most potent PA with MIC of 8 and 4 for *E. coli* and *S. aureus*, respectively. Notably, the MRSA strain was inhibited 30 - 37% with four of the neomycin PAs and up to 52% with DPA 1281 at 64  $\mu\text{M}$ .

2.8. Docking studies of kanamycin/neomycin conjugates with model *E. coli* A site RNA

Molecular docking studies were performed with few of the conjugates binding to bacterial A-site model RNA. The model (PDB 1pbr) used was the A-site of *E. coli* 16S ribosomal RNA.<sup>57</sup> The docking studies were performed with two kanamycin conjugates (Kan LY and Kan CV) and two neomycin conjugates (Neo LY and Neo CV) which showed significant change in melting temperature ( $T_m$ ) in UV denaturation experiments Figure 14. Analysis of the docked structures reveals that number of interactions (hydrogen bonding, van der Waals) between amino acid side chains of neomycin conjugates with *E. coli* A-site RNA are much more pronounced compared to that of kanamycin conjugates. Both the neomycin conjugates (Neo LY and Neo CV) fit well inside the grooves of A-site RNA, and the hydroxy group of tyrosine residue in Neo LY makes a close H-bond contact with phosphate backbone between U5 and C6. In contrast, the structure of Kan LY leaves tyrosine residue orienting away from the groove, leaving the hydroxyl group far from the backbone.

**Figure 14.** Docked structures of A-site bacterial RNA binding with (a) Kan LY (DPA 2060); (b) Kan CV (DPA 2081); (c) Neo LY (DPA 1261) and (d) Neo CV (DPA 1281)

### 3. Conclusion

A 210-member library of peptidic-kanamycin/neomycin conjugates was successfully synthesized via a rapid and efficient solid-phase protocol for developing DNA/RNA-targeted therapeutics. Various mono- and di-amino acid kanamycin/neomycin conjugates were rapidly synthesized. As compared to the synthesis of neomycin acid monomer **9**, synthesis of kanamycin acid monomer **6** resulted in the formation of various side products upon prolonged exposure to the atmosphere. However, subtle change in the reaction solvent conditions allowed us to isolate pure kanamycin amine within 2h which was then immediately coupled with succinic anhydride to afford kanamycin acid monomer **6** as the key precursor for the solid phase synthesis. The data suggest that for the examples studied here, the amino acid variations do not lead to a significant perturbation in the electronic behavior of the core aminoglycoside ring, allowing it to retain its specificity in binding and function.

Thermal denaturation analysis of PAs bound to human and *E. coli* A-site rRNA identified several kanamycin and neomycin peptidic conjugates that improved rRNA stability as compared to kanamycin or neomycin alone demonstrating the utility of our approach in modulating rRNA binding by simple amino acid variations. Molecular docking studies of select peptidic conjugates bound to the model bacterial A-site rRNA accurately predicted differential binding stabilities of neomycin PAs as compared to kanamycin PAs. These observations corroborated with the significant antibacterial activity of the neomycin PAs against aminoglycoside sensitive *S. aureus* and *E. coli*. Broader antibacterial screens and synergy profiles of these peptidic kanamycin- and neomycin conjugates on several Gram-positive and Gram-negative bacterial strains and their binding affinities for the bacterial 16S ribosomal A-site RNA using high-throughput screening are currently underway in our laboratory and will be reported in due course.

Previous approaches to synthesize modified aminoglycosides in our hands and from other groups have been performed in solution phase. A typical output for such solution phase reactions is ~1 compound per week per person, and would be significantly more time consuming, if multiple amino acids or fragments were attached to the aminoglycoside. Using a non-automated solid phase synthesis setup, we are able to synthesize up to 10 compounds per week per person, yielding a ten-fold improvement in output, in addition to the savings of solvent and silica needed for column purification. As more complex conjugates are synthesized and automation is considered, the increase in output could be further expanded to orders of magnitude. The rapid approach described in this work for solid-phase synthesis of various modified aminoglycoside conjugates and high-throughput screening could pave the way for identifying the optimal peptide chain residues and linker length required for developing novel antibiotics against bacterial, viral, and fungal pathogens containing potential nucleic acid binding sites.

### 4. Experimental section

**General information.** Solvents were dried and distilled according to literature procedures. Chemicals were purchased from commercial sources and were used without further purifications. Silica gel (100-200 mesh and 230-400 mesh) was used for column chromatography and TLC analysis was performed on commercial plates coated with silica gel 60 F<sub>254</sub>. Visualization of the spots on TLC plates was achieved by UV radiation or spraying ethanolic solution of ninhydrin and acetic acid. Mass spectra were obtained from Q-TOF instrument by Matrix

Assisted Laser Desorption/Ionization (MALDI). <sup>1</sup>H and <sup>13</sup>C NMR spectral analyses were performed on a spectrometer operating at 300 MHz, 500 MHz, and 75 MHz, 125 MHz, respectively in D<sub>2</sub>O solutions unless otherwise stated. Chemical shifts are reported with respect to solvent residual water peak at 4.79 ppm for <sup>1</sup>H NMR. Coupling constants (*J*) are reported in Hz. Standard abbreviations s, d, t, dd, br s, app s, m refer to singlet, doublet, triplet, doublet of doublet, broad singlet, apparent singlet, multiplet, respectively.

#### Antibacterial Screening and Minimal Inhibitory Concentration (MIC) Determination.

Initial screening of the library of kanamycin-peptide conjugates and neomycin-peptide conjugates against exponential phase microbial cultures was performed at single point concentration of 12.5 μM and 6.25 μM respectively, in duplicate wells using 96-well polystyrene microplates along with the reference compounds kanamycin or neomycin sulfate and kanamycin or neomycin acids. The same volume (10 μL) of sterile water with 1% DMSO was used for antibiotic addition was added to the broth (background control) and microbial culture (growth control). Plates were incubated in a humidified incubator at 37°C for 15-20 hours. The percent growth inhibition was calculated using the formula:

$$\% \text{ Growth Inhibition} = 100 - 100 \times \frac{A_{\text{compound}} - A_{\text{background}}}{A_{\text{control}} - A_{\text{background}}}$$

MIC values for select kanamycin-peptide conjugates and neomycin-peptide conjugates were determined for exponential phase bacterial cultures by the microdilution method in triplicate according to the Clinical Laboratory Standards protocol. Stock test compounds were prepared at ten times the final concentration in 10% dimethylsulfoxide (DMSO) followed by a serial 1:2 dilution. For each dilution, a ten-microliter aliquot of stock test compound was combined with 90 μl diluted bacterial suspension (~3 × 10<sup>5</sup> cells per mL) in cation-adjusted Mueller-Hinton broth. Final test compound concentrations from serial 2-fold dilutions ranged from 64 μM to 1 μM. Plates were incubated in a humidified incubator at 37°C for 15-20 h. After incubation with test compound, growth was measured by absorbance at 595 nm using a TecanM100Pro plate reader. The percent growth inhibition at each concentration was averaged from triplicate assays calculated from the formula above.

#### 4.1. Kanamycin acid derivative (**10**).

To a solution of compound **6** (0.1g, 0.102 mmol) in dichloromethane (1 mL) trifluoroacetic acid (0.5 mL) was added and stirred at room temperature for 3 h. The solvent was removed under vacuum and the residue was dissolved in deionized water (2 mL) and washed with ethyl acetate (3 × 10 mL). Lyophilization of the aqueous solution produced deprotected kanamycin acid derivative **10**, as a white solid powder (0.055 g, 92%); <sup>1</sup>H NMR (D<sub>2</sub>O, 300 MHz) δ 5.68 (d, *J* = 3.9 Hz, 1 H), 5.09 (d, *J* = 3.3 Hz, 1 H), 3.96-3.75 (m, 7 H), 3.67-3.32 (m, 9 H), 3.20-3.13 (m, 1 H), 2.63 (d, *J* = 6.6 Hz, 2 H), 2.55 (d, *J* = 5.7 Hz, 2 H), 2.06-1.97 (m, 1 H), 1.32-1.23 (m, 1 H); <sup>13</sup>C NMR (D<sub>2</sub>O, 75 MHz) δ 175.55, 163.22, 162.75, 118.26, 114.40, 100.70, 96.77, 83.62, 77.62, 73.33, 71.89, 71.04, 70.97, 70.80, 68.71, 68.13, 66.66, 54.66, 49.95, 48.14, 40.45, 39.23, 30.42, 29.64, 27.52; MS (MALDI-TOF) *m/z* calcd for C<sub>22</sub>H<sub>42</sub>N<sub>5</sub>O<sub>13</sub> [M + H]<sup>+</sup> 584.3, found 584.4.

#### 4.2. Kan CV (DPA 2081).

$^1\text{H}$  NMR ( $\text{D}_2\text{O}$ , 500 MHz)  $\delta$  5.62 (d,  $J = 4$  Hz, 1 H), 5.07 (app s, 1 H), 4.54-4.52 (m, 1 H), 4.12-4.10 (m, 1 H), 3.98-3.91 (m, 6 H), 3.78-3.68 (m, 5 H), 3.59-3.45 (m, 6 H), 3.20-3.14 (m, 3 H), 2.62-2.59 (m, 4 H), 2.00-1.93 (m, 1 H), 1.26-1.24 (m, 1 H), 0.95 (d,  $J = 6.5$  Hz, 6 H);  $^{13}\text{C}$  NMR ( $\text{D}_2\text{O}$ , 75 MHz)  $\delta$  175.92, 175.01, 173.88, 172.21, 163.23, 162.76, 118.26, 114.39, 100.78, 97.07, 83.69, 78.41, 75.71, 75.17, 72.02, 70.79, 68.73, 67.99, 66.66, 65.12, 59.41, 55.57, 54.70, 54.34, 49.98, 47.97, 44.52, 42.52, 40.31, 29.73, 27.54, 25.22, 17.68, 16.21; MS (MALDI-TOF)  $m/z$  calcd for  $\text{C}_{30}\text{H}_{57}\text{N}_8\text{O}_{14}\text{S}$  [ $\text{M} + \text{H}$ ] $^+$  785.4, found 785.6.

#### 4.3. Kan FV (DPA 2075)

$^1\text{H}$  NMR ( $\text{D}_2\text{O}$ , 300 MHz)  $\delta$  7.37-7.23 (m, 5 H), 5.56 (d,  $J = 3.6$  Hz, 1 H), 5.03 (d,  $J = 3.3$  Hz, 1 H), 4.58 (t,  $J = 7.5$  Hz, 1 H), 4.00-3.85 (m, 6 H), 3.76-3.66 (m, 3 H), 3.58-3.37 (m, 8 H), 3.23-3.16 (m, 2 H), 3.04 (d,  $J = 7.5$  Hz, 1 H), 2.84 (s, 1 H), 2.50 (app s, 4 H), 2.00-1.93 (m, 1 H), 1.25-1.22 (m, 1 H), 0.88 (d,  $J = 6.6$  Hz, 6 H);  $^{13}\text{C}$  NMR ( $\text{D}_2\text{O}$ , 75 MHz)  $\delta$  175.37, 175.24, 174.57, 173.24, 163.21, 162.74, 162.27, 136.13, 129.14, 128.79, 127.24, 118.26, 114.39, 110.53, 100.78, 97.06, 83.63, 78.80, 72.92, 72.02, 70.92, 70.77, 70.59, 68.74, 68.11, 66.57, 59.18, 55.19, 54.69, 54.34, 49.94, 47.87, 40.21, 39.23, 37.07, 30.57, 30.37, 29.84, 27.57, 18.26, 17.52; MS (MALDI-TOF)  $m/z$  calcd for  $\text{C}_{36}\text{H}_{61}\text{N}_8\text{O}_{14}$  [ $\text{M} + \text{H}$ ] $^+$  829.4, found 829.6.

#### 4.4. Kan VY (DPA 2066)

$^1\text{H}$  NMR ( $\text{D}_2\text{O}$ , 500 MHz)  $\delta$  7.16 (d,  $J = 8.5$  Hz, 2 H), 6.82 (d,  $J = 8$  Hz, 2 H), 5.57 (s, 1 H), 5.05 (s, 1 H), 4.58-4.54 (m, 1 H), 3.98-3.88 (m, 6 H), 3.77-3.70 (m, 2 H), 3.60-3.33 (m, 9 H), 3.22-3.14 (m, 3 H), 2.93-2.88 (m, 1 H), 2.60-2.52 (m, 4 H), 1.96-1.91 (m, 1 H), 1.28-1.21 (m, 1 H), 0.75 (d,  $J = 5$  Hz, 6 H);  $^{13}\text{C}$  NMR ( $\text{D}_2\text{O}$ , 125 MHz)  $\delta$  175.71, 175.56, 175.26, 173.54, 163.41, 163.12, 162.84, 154.33, 130.48, 128.46, 117.47, 115.45, 115.15, 112.83, 100.81, 97.25, 83.66, 78.64, 73.12, 71.95, 70.96, 70.74, 70.58, 68.70, 68.10, 66.60, 59.95, 54.72, 54.58, 54.33, 49.92, 47.92, 40.21, 39.20, 35.91, 30.51, 30.21, 29.60, 27.58, 18.06, 17.17; MS (MALDI-TOF)  $m/z$  calcd for  $\text{C}_{36}\text{H}_{61}\text{N}_8\text{O}_{15}$  [ $\text{M} + \text{H}$ ] $^+$  845.4, found 845.6.

#### 4.5. Kan LY (DPA 2060)

$^1\text{H}$  NMR ( $\text{D}_2\text{O}$ , 300 MHz)  $\delta$  7.14 (d,  $J = 8.7$  Hz, 2 H), 6.82 (d,  $J = 8.4$  Hz, 2 H), 5.56 (d,  $J = 3.6$  Hz, 1 H), 5.04 (d,  $J = 2.4$  Hz, 1 H), 4.55 (dd,  $J = 5.4$  Hz,  $J = 10.2$  Hz, 1 H), 4.10 (dd,  $J = 5.7$  Hz,  $J = 9.3$  Hz, 1 H), 3.97-3.84 (m, 5 H), 3.77-3.67 (m, 2 H), 3.60-3.31 (m, 8 H), 3.22-3.14 (m, 3 H), 2.92-2.83 (m, 1 H), 2.54-2.50 (m, 4 H), 1.95-1.82 (m, 1 H), 1.46-1.39 (m, 3 H), 1.27-1.22 (m, 1 H), 0.82 (d,  $J = 6.3$  Hz, 3 H), 0.77 (d,  $J = 6.3$  Hz, 3 H);  $^{13}\text{C}$  NMR ( $\text{D}_2\text{O}$ , 75 MHz)  $\delta$  175.73, 175.42, 175.21, 174.73, 163.21, 162.74, 154.33, 130.51, 128.47, 118.26, 115.40, 114.39, 100.81, 97.27, 83.65, 78.70, 73.11, 71.96, 70.97, 70.76, 70.58, 68.71, 68.11, 66.60, 54.73, 54.34, 52.96, 49.94, 47.94, 40.22, 39.50, 39.21, 35.82, 30.48, 30.24, 27.59, 24.12, 21.87, 20.72; MS (MALDI-TOF)  $m/z$  calcd for  $\text{C}_{37}\text{H}_{63}\text{N}_8\text{O}_{15}$  [ $\text{M} + \text{H}$ ] $^+$  859.4, found 859.6.

#### 4.6. Kan TD (DPA 1966)

$^1\text{H}$  NMR ( $\text{D}_2\text{O}$ , 300 MHz)  $\delta$  5.65 (d,  $J = 3.6$  Hz, 1 H), 5.07 (d,  $J = 2.7$  Hz, 1 H), 4.72 (t,  $J = 6.3$  Hz, 1 H), 4.30-4.23 (m, 5 H), 3.94-3.87 (m, 4 H), 3.84-3.70 (m, 2 H), 3.57-3.37 (m, 6 H), 3.19-3.13 (m, 2 H), 2.94-2.86 (m, 2 H), 2.68-2.65 (m, 4 H), 2.03-1.95

(m, 1 H), 1.23-1.22 (m, 1 H), 1.19 (d,  $J = 6$  Hz, 3 H);  $^{13}\text{C}$  NMR ( $\text{D}_2\text{O}$ , 75 MHz)  $\delta$  176.47, 175.67, 174.78, 174.27, 172.13, 163.21, 162.74, 118.25, 114.39, 100.72, 97.05, 83.70, 78.14, 71.96, 70.84, 68.73, 68.19, 66.75, 66.66, 59.34, 54.34, 52.33, 49.86, 44.52, 42.52, 40.70, 35.29, 30.47, 29.86, 29.00, 18.72; MS (MALDI-TOF)  $m/z$  calcd for  $\text{C}_{30}\text{H}_{55}\text{N}_8\text{O}_{17}$  [ $\text{M} + \text{H}$ ] $^+$  799.4, found 799.6.

#### 4.7. Neomycin acid derivative (II)

To a solution of compound **9** (0.1g, 0.076 mmol) in dichloromethane (1 mL) trifluoroacetic acid (0.5 mL) was added and stirred at room temperature for 3 h. The solvent was removed under vacuum and the residue was dissolved in deionized water (2 mL) and washed with ethyl acetate ( $3 \times 10$  mL). Lyophilization of the aqueous solution produced deprotected neomycin acid derivative **11**, as a white solid powder (0.048 g, 88%);  $^1\text{H}$  NMR ( $\text{D}_2\text{O}$ , 300 MHz)  $\delta$  5.89 (app s, 1 H), 5.34 (d,  $J = 3.6$  Hz, 1 H), 5.26 (s, 1 H), 4.35-4.19 (m, 5 H), 4.12-4.05 (m, 2 H), 4.02-3.85 (m, 2 H), 3.80 (s, 1 H), 3.75-3.33 (m, 12 H), 2.65-2.45 (m, 5 H), 1.95-1.82 (m, 1 H);  $^{13}\text{C}$  NMR ( $\text{D}_2\text{O}$ , 75 MHz)  $\delta$  178.80, 175.92, 163.56, 163.09, 162.62, 162.15, 122.11, 118.24, 114.38, 110.51, 109.13, 95.69, 94.92, 84.82, 80.82, 77.04, 75.23, 73.38, 72.16, 70.20, 70.08, 69.95, 68.04, 67.58, 67.39, 53.11, 50.77, 49.53, 48.47, 40.71, 40.44, 39.85, 31.01, 30.70, 27.88; MS (MALDI-TOF)  $m/z$  calcd for  $\text{C}_{27}\text{H}_{52}\text{N}_7\text{O}_{15}$  [ $\text{M} + \text{H}$ ] $^+$  714.4, found 714.6.

#### 4.8. Neo CV (DPA 1281)

$^1\text{H}$  NMR ( $\text{D}_2\text{O}$ , 300 MHz)  $\delta$  5.96 (s, 1 H), 5.38 (s, 1 H), 5.27 (s, 1 H), 4.53 (t,  $J = 6.3$  Hz, 1 H), 4.34-4.22 (m, 5 H), 4.10-3.92 (m, 5 H), 3.82 (s, 1 H), 3.76-3.69 (m, 2 H), 3.58-3.35 (m, 11 H), 2.90 (d,  $J = 5.7$  Hz, 2 H), 2.63-2.48 (m, 5 H), 1.96-1.83 (m, 1 H), 0.94 (d,  $J = 6.9$  Hz, 6 H);  $^{13}\text{C}$  NMR ( $\text{D}_2\text{O}$ , 75 MHz)  $\delta$  175.84, 175.30, 174.76, 172.16, 163.17, 162.70, 118.26, 114.40, 110.53, 109.39, 95.77, 94.89, 84.85, 80.61, 77.32, 75.21, 73.37, 72.26, 70.29, 70.15, 69.89, 68.10, 67.56, 67.35, 59.43, 55.46, 53.17, 50.81, 49.54, 48.49, 41.35, 40.48, 39.96, 30.62, 30.26, 29.78, 27.86, 25.40, 18.33, 17.61; MS (MALDI-TOF)  $m/z$  calcd for  $\text{C}_{35}\text{H}_{67}\text{N}_{10}\text{O}_{16}\text{S}$  [ $\text{M} + \text{H}$ ] $^+$  915.4, found 915.5.

#### 4.9. Neo FV (DPA 1276)

$^1\text{H}$  NMR ( $\text{D}_2\text{O}$ , 300 MHz)  $\delta$  7.35-7.22 (m, 5 H), 5.95 (s, 1 H), 5.37 (s, 1 H), 5.26 (s, 1 H), 4.58 (t,  $J = 7.5$  Hz, 1 H), 4.31-4.21 (m, 5 H), 4.10-3.97 (m, 5 H), 3.81 (s, 1 H), 3.74-3.67 (m, 2 H), 3.58-3.38 (m, 11 H), 3.03 (d,  $J = 7.2$  Hz, 2 H), 2.53-2.50 (m, 5 H), 1.96-1.92 (m, 1 H), 0.88 (d,  $J = 6.6$  Hz, 6 H);  $^{13}\text{C}$  NMR ( $\text{D}_2\text{O}$ , 75 MHz)  $\delta$  175.29, 175.24, 174.36, 173.24, 163.17, 162.70, 162.23, 136.09, 129.15, 128.80, 127.27, 118.26, 114.39, 109.39, 95.76, 94.88, 84.83, 80.58, 77.35, 75.21, 73.37, 72.25, 70.28, 70.14, 69.88, 68.08, 67.55, 67.35, 59.19, 55.20, 54.34, 53.16, 50.80, 49.54, 48.48, 40.46, 39.94, 37.18, 30.63, 30.23, 29.89, 27.87, 18.23, 17.55; MS (MALDI-TOF)  $m/z$  calcd for  $\text{C}_{41}\text{H}_{71}\text{N}_{10}\text{O}_{16}$  [ $\text{M} + \text{H}$ ] $^+$  959.5, found 959.7.

#### 4.10. Neo VY (DPA 1267)

$^1\text{H}$  NMR ( $\text{D}_2\text{O}$ , 500 MHz)  $\delta$  7.15 (d,  $J = 8$  Hz, 2 H), 6.83 (d,  $J = 8.5$  Hz, 2 H), 5.96 (s, 1 H), 5.39 (s, 1 H), 5.28 (s, 1 H), 4.57-4.54 (m, 1 H), 4.35-4.22 (m, 5 H), 4.13-3.93 (m, 5 H), 3.82 (s, 1

H), 3.73-3.70 (m, 2 H), 3.62-3.34 (m, 11 H), 3.20-3.09 (m, 2 H), 2.60-2.49 (m, 5 H), 1.95-1.92 (m, 1 H), 0.80-0.77 (m, 6 H);  $^{13}\text{C}$  NMR ( $\text{D}_2\text{O}$ , 125 MHz)  $\delta$  175.57, 175.33, 174.95, 173.48, 163.37, 163.08, 162.80, 162.52, 154.38, 130.51, 128.25, 119.79, 117.47, 115.43, 115.15, 112.84, 109.45, 95.74, 94.89, 84.84, 80.49, 77.36, 75.24, 73.36, 72.25, 70.30, 70.13, 69.86, 68.08, 67.53, 67.33, 59.72, 54.57, 54.33, 53.15, 50.79, 49.54, 48.47, 40.45, 39.97, 36.12, 30.62, 30.15, 29.87, 27.85, 18.14, 17.34; MS (MALDI-TOF)  $m/z$  calcd for  $\text{C}_{41}\text{H}_{71}\text{N}_{10}\text{O}_{17}$   $[\text{M} + \text{H}]^+$  975.5, found 975.7.

#### 4.11. Neo LY (DPA 1261)

$^1\text{H}$  NMR ( $\text{D}_2\text{O}$ , 500 MHz)  $\delta$  7.14 (d,  $J = 8.5$  Hz, 2 H), 6.83 (d,  $J = 8.5$  Hz, 2 H), 5.96 (s, 1 H), 5.39 (s, 1 H), 5.28 (s, 1 H), 4.58-4.55 (m, 1 H), 4.35-4.22 (m, 5 H), 4.17-4.12 (m, 2 H), 4.02-3.92 (m, 3 H), 3.82 (s, 1 H), 3.72-3.69 (m, 2 H), 3.59-3.34 (m, 10 H), 3.20-3.13 (m, 2 H), 2.57-2.55 (m, 5 H), 1.94-1.87 (m, 1 H), 1.44-1.38 (m, 3 H), 0.84 (d,  $J = 6$  Hz, 3 H), 0.79 (d,  $J = 6$  Hz, 3 H);  $^{13}\text{C}$  NMR ( $\text{D}_2\text{O}$ , 125 MHz)  $\delta$  175.61, 175.31, 174.90, 174.69, 163.37, 163.09, 162.81, 154.36, 130.53, 128.27, 119.79, 117.48, 115.39, 115.16, 109.44, 95.75, 94.87, 84.82, 80.48, 77.38, 75.25, 73.35, 72.24, 70.29, 70.13, 69.86, 68.09, 67.53, 67.33, 54.33, 53.15, 52.79, 50.79, 49.54, 48.47, 42.51, 41.47, 40.45, 39.95, 39.65, 36.00, 30.57, 30.09, 27.84, 24.15, 21.85, 20.76; MS (MALDI-TOF)  $m/z$  calcd for  $\text{C}_{42}\text{H}_{73}\text{N}_{10}\text{O}_{17}$   $[\text{M} + \text{H}]^+$  989.6, found 989.8.

#### 4.12. Neo TD (DPA 1167)

$^1\text{H}$  NMR ( $\text{D}_2\text{O}$ , 500 MHz)  $\delta$  5.97 (s, 1 H), 5.40 (s, 1 H), 5.28 (s, 1 H), 4.73-4.70 (m, 1 H), 4.36-4.24 (m, 7 H), 4.13-4.10 (m, 1 H), 4.03-3.94 (m, 3 H), 3.83 (s, 1 H), 3.73-3.68 (m, 2 H), 3.55-3.37 (m, 10 H), 2.96-2.92 (m, 1 H), 2.88-2.86 (m, 1 H), 2.69-2.68 (m, 4 H), 2.60-2.59 (m, 1 H), 1.94-1.87 (m, 1 H), 1.20 (d,  $J = 6$  Hz, 3 H);  $^{13}\text{C}$  NMR ( $\text{D}_2\text{O}$ , 125 MHz)  $\delta$  176.96, 175.38, 174.82, 174.48, 172.08, 163.37, 163.08, 162.80, 162.51, 119.80, 117.47, 115.15, 112.83, 109.40, 95.73, 94.88, 84.81, 80.51, 77.29, 75.21, 73.34, 72.23, 70.25, 70.14, 69.85, 68.10, 67.55, 67.34, 66.87, 66.74, 59.15, 54.33, 53.16, 50.78, 49.97, 48.47, 40.46, 39.93, 35.63, 30.56, 29.87, 29.00, 27.85, 18.72; MS (MALDI-TOF)  $m/z$  calcd for  $\text{C}_{35}\text{H}_{65}\text{N}_{10}\text{O}_{19}$   $[\text{M} + \text{H}]^+$  929.4, found 929.6.

**UV thermal denaturation experiments.** UV thermal denaturation experiments were carried out using a Cary 100E UV-Vis spectrophotometer with a thermoelectrically controlled 12-cell holder. The stability of spectrophotometer and wavelength alignment were checked prior to initiation of each UV experiment. The samples were prepared by dilution of a stock RNA sample that was prepared by heating the RNA to 95 °C for 10 minutes, followed by slow cooling to room temperature. The samples were incubated at 4 °C for 12 h, followed by the addition of ligands in 1:1 molar ratio and kept at 4 °C for another 1 h. All the samples were analyzed in quartz cells of 1 cm path length. All UV experiments were monitored at 260 nm, conducted at a heating rate of 0.2 °C/min, data were recorded every 1 °C interval and melting temperature was determined by sigmoidal fitting analysis in origin software. The buffer used in the preparation of samples was HEPES-NaCl buffer (10 mM HEPES, 50 mM NaCl, 0.09 mM EDTA in DEPC-treated  $\text{H}_2\text{O}$ , pH 7.0).

**Molecular docking experiments.** Molecular docking experiments were performed using AutoDock Vina.<sup>58</sup> Prepared pdb files of the ligands and receptor were provided to AutoDock tools to get

the corresponding pdbqt files. The pdb file (1pbr)<sup>60</sup> of the receptor bacterial A-site RNA was taken from Protein Data Bank and prepared for docking by deleting the bound ligand. Final figures of the docked structures were made by using PyMol.

#### Acknowledgments

We thank the National Institutes of Health for financial support (grants R42GM097917, AI114114) to DPA.

#### References and notes

1. Moazed, D.; Noller, H. F. *Nature* **1987**, *6121*, 389-394.
2. Arya, D. P. In *Aminoglycoside Antibiotics: From Chemical Biology to Drug Discovery*. Wang, B., Ed.; - John Wiley & Sons, Inc.: 2007; pp - 319 pp.
3. Willis, B.; Arya, D. P. *Adv. Carbohydr. Chem. Biochem.* **2006**, 251-302.
4. Chambers, H. F.; DeLeo, F. R. *Nat. Rev. Microbiol.* **2009**, *9*, 629-641.
5. Husain, N.; Tkaczuk, K. L.; Tulsidas, S. R.; Kaminska, K. H.; Cubrilo, S.; Maravic-Vlahovicek, G.; Bujnicki, J. M.; Sivaraman, J. *Nucleic Acids Res.* **2010**, *12*, 4120-4132.
6. Busscher, G. F.; Rutjes, F. P.; van Delft, F. L. *Chem. Rev.* **2005**, *3*, 775-791.
7. Aggen, J. B.; Armstrong, E. S.; Goldblum, A. A.; Dozzo, P.; Linsell, M. S.; Gliedt, M. J.; Moser, H. E.

- Antimicrobial Agents and Chemotherapy* **2010**, 4636-4642.
8. Bera, S.; Zhanel, G. G.; Schweizer, F. *Bioorg. Med. Chem. Lett.* **2010**, 10, 3031-3035.
9. Bera, S.; Zhanel, G. G.; Schweizer, F. *J. Med. Chem.* **2010**, Copyright (C) 2012 American Chemical Society (ACS). All Rights Reserved., 3626-3631.
10. Findlay, B.; Zhanel, G. G.; Schweizer, F. *Bioorg. Med. Chem. Lett.* **2012**, 4, 1499-1503.
11. Bera, S.; Dhondikubeer, R.; Findlay, B.; Zhanel, G. G.; Schweizer, F. *Molecules* **2012**, 8, 9129-9141.
12. Zhang, J.; Chiang, F. I.; Wu, L.; Czyryca, P. G.; Li, D.; Chang, C. W. *J. Med. Chem.* **2008**, 23, 7563-7573.
13. Fridman, M.; Belakhov, V.; Yaron, S.; Baasov, T. *Org. Lett.* **2003**, 20, 3575-3578.
14. Hainrichson, M.; Pokrovskaya, V.; Shallom-Shezifi, D.; Fridman, M.; Belakhov, V.; Shachar, D.; Yaron, S.; Baasov, T. *Bioorg. Med. Chem.* **2005**, 20, 5797-5807.
15. Kling, D.; Heseck, D.; Shi, Q.; Mobashery, S. *J. Org. Chem.* **2007**, 14, 5450-5453.
16. Asensio, J. L.; Hidalgo, A.; Bastida, A.; Torrado, M.; Corzana, F.; Chiara, J. L.; Garcia-Junceda, E.; Canada, J.; Jimenez-Barbero, J. *J. Am. Chem. Soc.* **2005**, 23, 8278-8279.
17. Quader, S.; Boyd, S. E.; Jenkins, I. D.; Houston, T. A. *J. Org. Chem.* **2007**, 6, 1962-1979.
18. Li, J.; Chiang, F. I.; Chen, H. N.; Chang, C. W. *J. Org. Chem.* **2007**, 11, 4055-4066.
19. Shaul, P.; Green, K. D.; Rutenberg, R.; Kramer, M.; Berkov-Zrihen, Y.; Breiner-Goldstein, E.; Garneau-Tsodikova, S.; Fridman, M. *Org. Biomol. Chem.* **2011**, 11, 4057-4063.
20. Fosso, M. Y.; Zhu, H.; Green, K. D.; Garneau-Tsodikova, S.; Fredrick, K. *Chembiochem* **2015**, 11, 1565-1570.
21. Herzog, I. M.; Green, K. D.; Berkov-Zrihen, Y.; Feldman, M.; Vidavski, R. R.; Eldar-Boock, A.; Satchi-Fainaro, R.; Eldar, A.; Garneau-Tsodikova, S.; Fridman, M. *Angew. Chem. Int. Ed Engl.* **2012**, 23, 5652-5656.
22. Shrestha, S. K.; Fosso, M. Y.; Green, K. D.; Garneau-Tsodikova, S. *Antimicrob. Agents Chemother.* **2015**, 8, 4861-4869.
23. Hanessian, S.; Szychowski, J.; Adhikari, S. S.; Vasquez, G.; Kandasamy, P.; Swayze, E. E.; Migawa, M. T.; Ranken, R.; Francois, B.; Wirmer-Bartoschek, J.; Kondo, J.; Westhof, E. *J. Med. Chem.* **2007**, 10, 2352-2369.

24. Pokrovskaya, V.; Belakhov, V.; Hainrichson, M.; Xue, L.; Xi, H.; Kumar, S.; Gray, D.; Davis, E.; Yaron, S.; Baasov, T. *J. Med. Chem.* **2009**, *8*, 2243-2254.
25. Arya, D. P.; Willis, B. *J. Am. Chem. Soc.* **2003**, *41*, 12398-12399.
26. Arya, D. P.; Xue, L.; Tennant, P. *J. Am. Chem. Soc.* **2003**, *27*, 8070-8071.
27. Willis, B.; Arya, D. P. *Biochemistry* **2006**, *34*, 10217-10232.
28. Watkins, D.; Jiang, L.; Nahar, S.; Maiti, S.; Arya, D. P. *PLoS One* **2015**, *12*, e0144251.
29. Watkins, D.; Norris, F. A.; Kumar, S.; Arya, D. P. *Anal. Biochem.* **2013**, *2*, 300-307.
30. Xi, H.; Davis, E.; Ranjan, N.; Xue, L.; Hyde-Volpe, D.; Arya, D. P. *Biochemistry* **2011**, *42*, 9088-9113.
31. Willis, B.; Arya, D. P. *Biochemistry-Us* **2010**, *3*, 452-469.
32. Willis, B.; Arya, D. P. *Bioorg. Med. Chem. Lett.* **2009**, *17*, 4974-4979.
33. Xue, L.; Charles, I.; Arya, D. P. *Chem. Commun. (Camb)* **2002**, *1*, 70-71.
34. Xue, L.; Xi, H.; Kumar, S.; Gray, D.; Davis, E.; Hamilton, P.; Skriba, M.; Arya, D. P. *Biochemistry* **2010**, *26*, 5540-5552.
35. Xue, L.; Xi, H.; Kumar, S.; Gray, D.; Davis, E.; Hamilton, P.; Skriba, M.; Arya, D. P. *Biochemistry* **2010**, *26*, 5540-5552.
36. Watkins, D.; Gong, C.; Kellish, P.; Arya, D. P. *Bioorg. Med. Chem.* **2017**, *4*, 1309-1319.
37. Shaw, N. N.; Xi, H.; Arya, D. P. *Bioorg. Med. Chem. Lett.* **2008**, *14*, 4142-4145.
38. Xi, H. J.; Kumar, S.; Dosen-Micovic, L.; Arya, D. P. *Biochimie* **2010**, *5*, 514-529.
39. Xue, L.; Ranjan, N.; Arya, D. P. *Biochemistry* **2011**, 2838-2849.
40. Ranjan, N.; Arya, D. P. *Molecules* **2013**, *11*, 14228-14240.
41. Ranjan, N.; Arya, D. P. *Bioorg. Med. Chem. Lett.* **2016**, *24*, 5989-5994.
42. Willis, B.; Arya, D. P. *Bioorg. Med. Chem.* **2014**, *7*, 2327-2332.
43. Nahar, S.; Ranjan, N.; Ray, A.; Arya, D. P.; Maiti, S. *Chemical Science* **2015**, *10*, 5837-5846.

44. Ranjan, N.; Kumar, S.; Watkins, D.; Wang, D.; Appella, D. H.; Arya, D. P. *Bioorg. Med. Chem. Lett.* **2013**, *20*, 5689-5693.
45. Kumar, S.; Arya, D. P. *Bioorg. Med. Chem. Lett.* **2011**, *16*, 4788-4792.
46. Kumar, S.; Ranjan, N.; Kellish, P.; Gong, C.; Watkins, D.; Arya, D. P. *Organic & biomolecular chemistry* **2016**, *6*, 2052-2056.
47. Watkins, D.; Kumar, S.; Green, K. D.; Arya, D. P.; Garneau-Tsodikova, S. *Antimicrob. Agents Chemother.* **2015**, *7*, 3899-3905.
48. Yi Jin, Derrick Watkins, Natalya N. Degtyareva, Keith D. Green, Meredith N. Spano, Sylvie Garneau-Tsodikova, and Dev P. Arya *med chem comm* **2015**.
49. Watkins, D.; Kumar, S.; Green, K. D.; Arya, D. P.; Garneau-Tsodikova, S. *Antimicrob. Agents Chemother.* **2015**, *7*, 3899-3905.
50. Charles, I.; Xi, H.; Arya, D. P. *Bioconjug. Chem.* **2007**, *1*, 160-169.
51. Charles, I.; Xue, L.; Arya, D. P. *Bioorg. Med. Chem. Lett.* **2002**, *9*, 1259-1262.
52. Charles, I.; Arya, D. P. *J. Carbohydr. Chem.* **2005**, Copyright (C) 2012 American Chemical Society (ACS). All Rights Reserved., 145-160.
53. Jiang, L.; Watkins, D.; Jin, Y.; Gong, C.; King, A.; Washington, A. Z.; Green, K. D.; Garneau-Tsodikova, S.; Oyelere, A. K.; Arya, D. P. *ACS Chem. Biol.* **2015**, *5*, 1278-1289.
54. Coin, I.; Beyermann, M.; Bienert, M. *Nature Protocols* **2007**, *12*, 3247-3256.
55. Cox, J. R.; Serpersu, E. H. *Carbohydr. Res.* **1995**, *1*, 55-63.
56. Reid, D. G.; Gajjar, K. *J. Biol. Chem.* **1987**, *17*, 7967-7972.
57. Fourmy, D.; Recht, M. I.; Blanchard, S. C.; Puglisi, J. D. *Science* **1996**, *5291*, 1367-1371.
58. Trott, O.; Olson, A. J. *J. Comput. Chem.* **2010**, 455-461.